ISSN 1068-3755, Surface Engineering and Applied Electrochemistry, 2021, Vol. 57, No. 1, pp. 117–123. © Allerton Press, Inc., 2021.

Enhanced Emission Properties of Anodized Polar ZnO Crystals

V. V. Zalamai[a, *], G. V. Colibaba[b], E. I. Monaico[a], and E. V. Monaico[a, **]

[a] *National Center for Materials Study and Testing, Technical University of Moldova, Chisinau, MD-2004 Moldova*

[b] *Moldova State University, Chisinau, MD-2009 Moldova*

**e-mail: victor.zalamai@cnstm.utm.md*

***e-mail eduard.monaico@cnstm.utm.md*

Received May 10, 2020; revised June 22, 2020; accepted June 22, 2020

Abstract– Polar ZnO single crystals were microstructured in a controlled fashion by electrochemical etching. Surfaces with pyramids and inversed pyramids on oxygen and zinc faces, respectively, were received. Photoluminescence spectra of bulk and anodized ZnO samples were investigated at room and low temperatures. Cathodoluminescence images were also recorded from areas with different structures. A significant enhancement of light emission of the prepared microstructures was achieved after anodization. This allows to use such microstructures in light emitting devices and solar cells.

Keywords: zinc oxide, anodization, morphology, pyramidal structures, photoluminescence, cathodoluminescence

DOI: 10.3103/S1068375521010166

INTRODUCTION

Zinc oxide (ZnO) is a direct bandgap semiconductor compound ($E_g = 3.37$ eV at $T = 300$ K) [1], which is of interest due to its wide band gap and a large binding energy of exciton at room temperature (60 meV). From the point of view of practical application, ZnO is a much cheaper material as compared to wide-bandgap GaN and InGaN. Nanostructures based on ZnO find wide applications in the development of electronic devices (light emitting- and laser-diodes) for blue and ultraviolet spectral ranges, gas sensors, and even in spintronic devices [2]. Solar cells are developed on *p*-ZnTe/*n*-ZnO heterojunctions [3].

Comprehensive investigations of photolu-minescence (PL), absorption and reflection properties of ZnO single crystals date back to the 1960s [4–7]. Since then, a huge amount of PL investigations of ZnO single crystals, layers, thin films, hetero-structures, and nanostructures have been carried out (for an overview see, e.g., the reviews and book chapters [1, 8–10] and references therein). Despite the comprehensive research and a large quantity of publications, several aspects still remain unclear and controversial. Among those, one can mention the assigning of certain exciton lines to donor or acceptor impurities, and the identification of their chemical nature.

Usually, the single crystals with better quality and a high uniformity of doping and electrical parameters are grown from the vapor phase [11, 12], for example, by chemical vapor transport (CVT). Unfortunately, the CVT technology for ZnO is still not well developed. The use of typical transport agents, such as H_2, C, and HCl, leads to the formation of voids in the crystals, high growth of nuclei density, and a very low growth rate, respectively [13–15]. Recently, new methods, based on HCl + H_2/CO/C transport agent mixtures, have been proposed for unseeded growth of ZnO single crystals, with the growth rates up to 1.5 mm per day, controllable shapes of crystals, and uniform doping by shallow Cl donor impurity achieved [16–18]. The free electron concentration in such crystals can be varied at least in a 4×10^{17}–5×10^{18} cm^{-3} range [19]. Complex transport agents based on HCl can be effective for the growth of ZnO crystals doped with many metallic impurities, including some transition metals and rare-earth elements [20, 21]. Such crystals are expected to be prospective luminescent materials for various spectral ranges.

The goal of this paper was to demonstrate a cost-effective approach, via anodization, for controlled micro-structuring of polar ZnO crystals with different luminescence properties, as well as the analysis of their light emission spectra. The present study should allow enhancement of the emission properties of the ZnO surface and offer a possibility to change spectral composition of luminescence in a wide range.

EXPERIMENTAL

Crystal Growth

ZnO crystals, with a hexagonal structure of wurtzite type, were grown by the CVT method using H_2

(2 atm) + HCl (2 atm) gas mixture as a transport agent, at growth temperature of 1020°C and undercooling at about 50°C [16]. The excess of Zn in the grown crystals was minimized by a post-growth annealing in air at 1000°C. This annealing essentially decreases the concentration of intrinsic donor defects, such as oxygen vacancies (V_O) and interstitial zinc (Zn_i), and increases the transparency of crystals in a visible spectral range [16]. The concentration of free electrons, measured from the temperature dependence of the Hall effect, was 3×10^{18} cm^{-3}, as reported in [19]. The grown material was cut into plates with 1 mm thickness. Those plates were polished with 1 μm diamond paste, followed by etching in an HCl aqueous solution and annealed in air to decrease a damaged layer generated by polishing. In all of the plates, the *c* axis of the hexagonal structure was oriented perpendicularly to the plate surface, hence the investigated surface corresponded to [0001] (Zn-face) or [000$\bar{1}$] (O-face) planes. The type of the surface was determined by the shape of pits, obtained by etching in acidic or alkaline solutions, as presented elsewhere [22].

Anodization

Electrochemical etching of the O-face or the Zn-face was carried out in a stirred 5% HCl aqueous solution for 2 min, in a potentiostatic mode, under different voltage biases. An electrical contact was made on the backside of the samples using a conductive silver paste. From the top side, the sample was pressed by an O-ring to leave a surface with an area of 0.2 cm^2 exposed to the electrolyte. The anodization of polar ZnO crystals was carried out in a common two-electrode cell, where the sample served as working electrode. A mesh with the surface of 6 cm^2 from platinum wire with 0.5 mm diameter was used as counter electrode. All experiments were performed inside a fume hood at room temperature. A Keithley's Series 2400 Source Measure Unit was used as potentiostat.

Characterization

A Vega Tescan 5130 MM Scanning Electron Microscope (SEM) equipped with an Oxford Instruments INCA Energy EDX system operated at 20 kV was used to investigate the morphology of anodized ZnO crystals. PL spectra were measured with a double high-aperture spectrometer SDL-1 (aperture 1 : 2, linear dispersion 7 A/mm), the ZnO samples being mounted on the cold finger of a closed cryogenic system LTS-382. The PL excitation was carried out by the 325 nm line radiation from a He-Cd laser. Cathodoluminescence (CL) images were collected using a Hamamatsu R943-02 high sensitivity photomultiplier tube (HSPMT). CL images were generated using a 10 keV, 10 nA electron beam. Note the working distance was ~ 12 mm due to the insertion of a CL paraboloidal mirror.

RESULTS AND DISCUSSIONS

Morphology Investigations

Figure 1 illustrates the morphologies of microstructures received by electrochemical etching process on the O-face (Figs. 1a, 1b) and on the Zn-face (Figs. 1c, 1d) of a ZnO crystal anodized at 5 V (Figs. 1a, 1c) and 10 V (Fig. 1b,d). One can see that, upon anodizing at 5 V, hexagonal pyramids with a diameter of the base around 1–5 μm were formed on the O-face of the ZnO crystal (see Fig. 1a). With increasing anodizing potential, the hexagonal pyramids become larger in diameter (Fig. 1b). On the other hand, hexagonal pits (inverted pyramids) are produced on the Zn-face (see Fig. 1c). With increasing of anodization potential to 10 V, those hexagonal pits are transformed into macropores consisting of stepped hexagonal pyramids, as shown in Fig. 1d. To note, that the formation of pyramidal structures and stepped hexagonal pits on O-face and Zn-face, respectively, was so far observed on ZnO and GaN thin films during wet chemical etching and reported in detail elsewhere [23, 24].

The electrochemical dissolution behaviors of ZnO on the O-face and on the Zn-face in a HCl solution was characterized by the *I–V* curves presented in Fig. 1e. Three regions with different slopes can be distinguished in the polarization curves for both investigated surfaces. At the beginning of anodization, a very low current level was registered in region I when the applied potential was lower than the breakdown potential or the pore formation potential estimated approximately at 3 V. As the potential is raised above 4 V, the anodic current first slowly increases, and above about 14 V the current rises steeply for the Zn-face. The beginning of region II was attributed to the formation of structures with small dimensions. A further increase in the applied voltage leads to the formation of structures with larger dimensions. At higher applied potentials, more than 14 V for the Zn-face (see region III') and more than 18 V for the O-face (see region III''), an isotropic electrochemical polishing was observed. The variations of the current during anodization depicted in Fig. 1f is explained by nucleation of the etch pits at the first stage followed by an exponential decrease of the current due to an increase of the pore depth and diffusion limitation of chemical species at the pore tips, especially for the Zn-face.

Photoluminescence Investigations

Figure 2a illustrates PL spectra of the ZnO samples anodized at 5 and 10 V on the O-face in comparison with those of the bulk ZnO O-face measured at room temperature. It can be clearly seen that the intensity of a spectrum is strongly influenced by the applied voltage during anodization. In the PL spectra measured at room temperature, two bands dominate. The first band is situated at 3.3 eV and can be associated with exciton recombination [9]. The broad band at 2.56 eV is

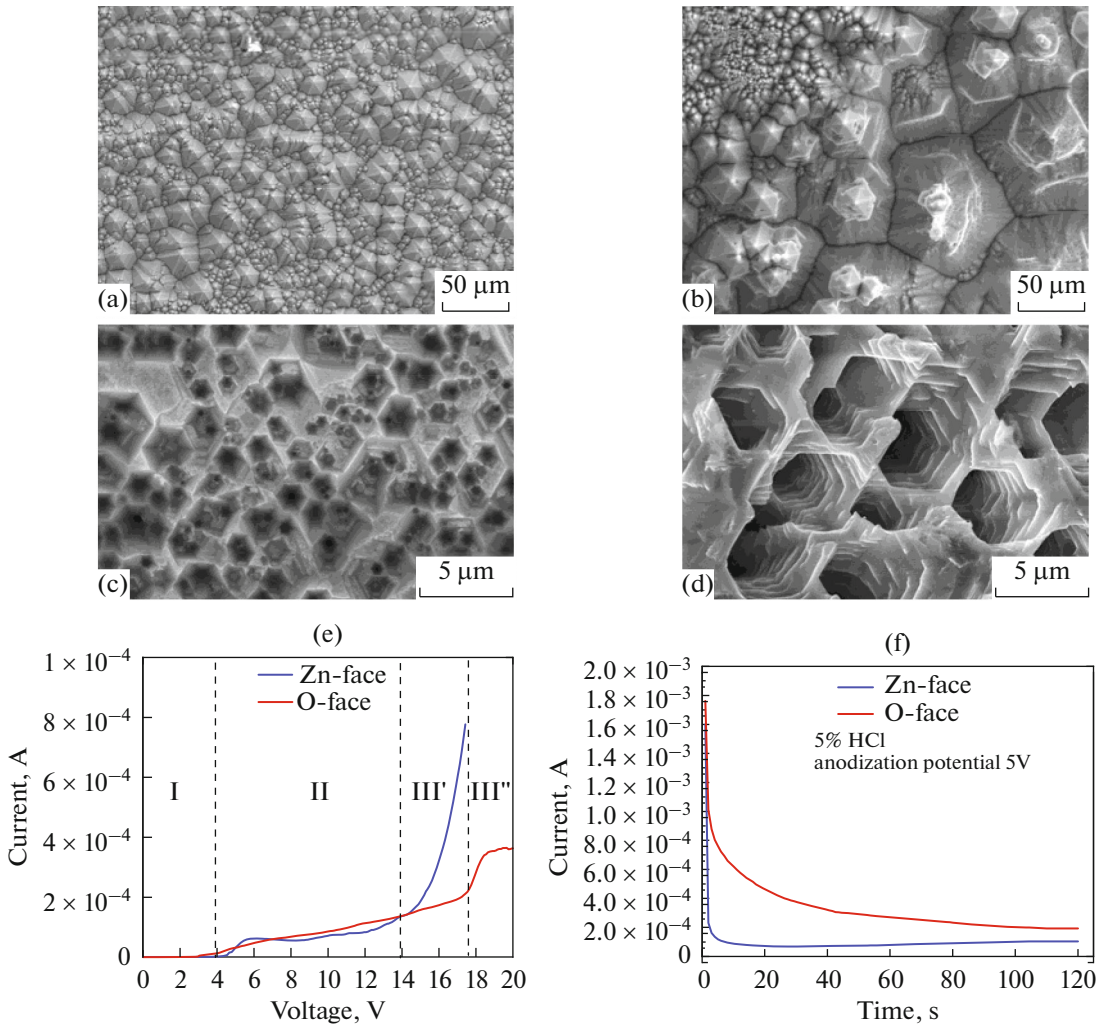

Fig. 1. SEM images of O-face (a, b) and Zn-face (c, d) of ZnO plates anodized in 5% HCl electrolyte at 5 V (a, c) and 10 V (b, d), respectively. The polarization curves measured at the beginning of the electrochemical etching of ZnO on both faces are presented in (e). Variations of the etching current during anodization of ZnO crystal on both faces at 5 V are in (f).

due to a typical for ZnO green luminescence [8, 9]. Usually this green luminescence is associated with uncontrollable impurities (Cu) and intrinsic defects (V_O) in ZnO [9]. Figure 2b illustrates the behavior of PL of the bulk and the anodized ZnO sample on the O-face at a low temperature (10 K). The observed picture is very similar to the case of the room temperature spectra. The most intensive band at 3.35 eV is situated in the ultraviolet region and can be attributed to the emission of excitons bound with neutral donors (D^0X) [10]. Another band, observed at 2.5 eV, is wider and is associated with the emission from uncontrollable defects [9].

The total efficiency of PL can be essentially enhanced after anodization (Fig. 2). It happens due to decreasing of nonradiative recombination canals generated by polishing and formation of surface microstructures of suitable size. The near edge emission dominates in the spectra of the morphology with small pyramids (see Fig. 1a), while *green* emission remains relatively weak. The morphology with big pyramids from Fig. 1b is characterized by relatively intensive green luminescence, but the near edge emission is weakened. Such influence of the surface morphology on PL spectra and on share of various bands is similar for both room and low temperatures.

ZnO demonstrates a great variety of photoluminescence lines covering almost the all visible and near ultraviolet spectral range from 2.0 to 3.5 eV. The most powerful PL is usually observed near the fundamental band edge with diverse lines especially at low temperatures. The PL spectrum in the excitonic region at 10 K of the anodized O-face at 5 V is shown in detail in Fig. 3. Four bands of PL due to excitons are situated at energies of 3.356 (D^0X_1), 3.360 (D^0X_2), 3.366 (D^0X_3), and 3.371 (FX_A) eV. FX_A is a well-known PL band of free excitons [9]. The most intensive D^0X_1 band is

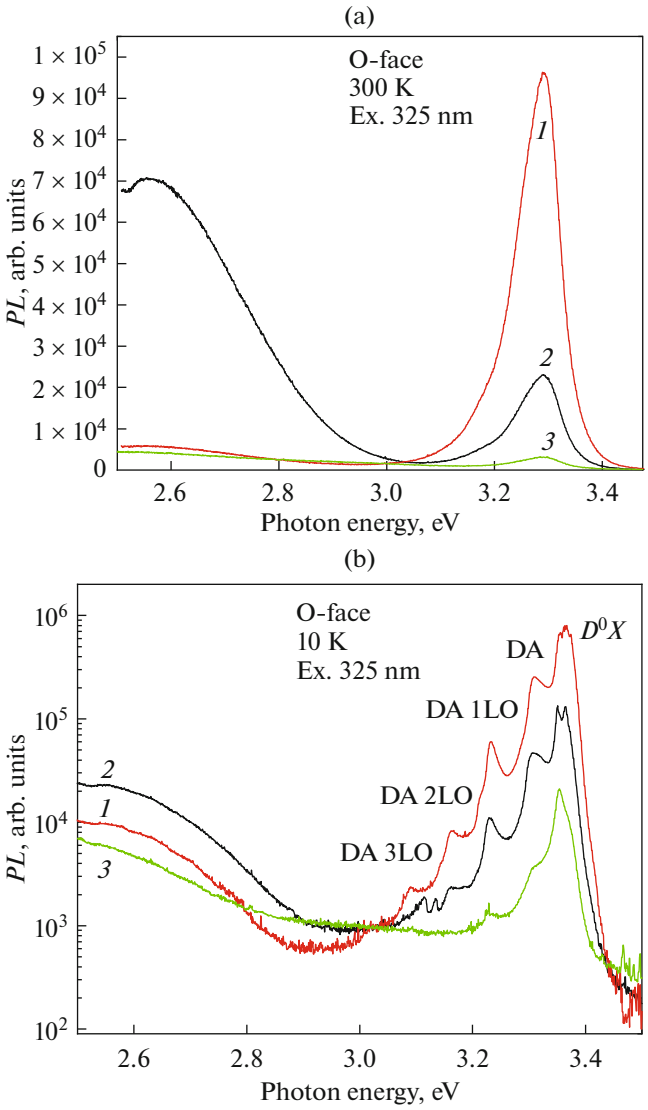

Fig. 2. PL spectra measured at: (a) room temperature and (b) at 10 K from O-face of ZnO plates before anodization (curve *3*), and after anodization at 5 V (curve *1*), and at 10 V (curve *2*).

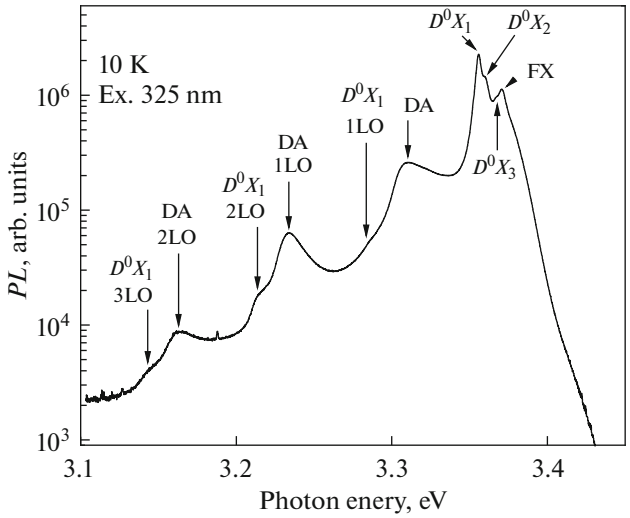

Fig. 3. PL spectra of ZnO crystal anodized at 5 V on O-face measured at 10 K.

attributed to excitons bound with dominating Cl donors with the activation energy of 38 ± 6 meV [10]. Positions of D^0X_2 and D^0X_3 lines correspond to photoluminescence associated with excitons bound with uncontrollable donors, which is usually observed in ZnO single crystals [25] and epitaxial layers [26]. Such donors can be In, Al, Ga, or Zn_i [27]. A broad band DA at 3.31 eV is one of those usually observed in high-quality ZnO epitaxial layers [28–32] and nanocrystalline films [33]. Different recombination channels were taken into account in order to explain this band. Initially, it was associated with a LO phonon replica of free excitons luminescence [26, 28–32] or with excitons bound at a neutral acceptor [28]. It is possible that the origin of these lines differs from a sample to a sample depending on the manufacturing technology. This DA band is associated with a donor–acceptor recombination as stated in [1, 8–10]. As reported in [19], this band is caused mainly by excitons bound with deep acceptors (600 meV), related to zinc vacancy-donor complex defects (Cl), which were predicted earlier in [34]. Other bands observed in a spectral range 3.1–3.3 eV can be attributed to longitudinal phonon replicas of bound excitons with the energy spacing of 72 meV.

There is no significant difference between PL spectra measured on both the O- and Zn-faces, only a very weak one was registered in the intensities of spectra. The PL spectrum from the O-face is a bit more intensive than that of the Zn-face as is illustrated in Fig. 4. Two bands with almost similar intensities (a green band located at ~2.5 eV and a red band at ~ 1.9 eV) dominate in these PL spectra at room temperature. The *red* emission shows the creation of charged oxygen vacancies (V_O^+), as stated in [35]. The *green* emission can be associated with oxygen vacancies (V_O) [36], zinc interstitial (Zn_i) [37], uncontrollable Cu [9], or surface defects [38]. A sharp intensive line observed in the spectra at ~1.9 eV is due to the second order of the excitation laser line.

Cathodoluminescence Investigations

In the presented here PL measurements, a sample with a special design was prepared by anodization of bulk ZnO on the O-face. First, a window with a large surface entering into a contact with the electrolyte was prepared, and the sample was subjected to anodization at 5 V. After that, a half of the window was covered by chemically stable epoxy and the remaining unprotected part of the window was etched at 10 V. As a

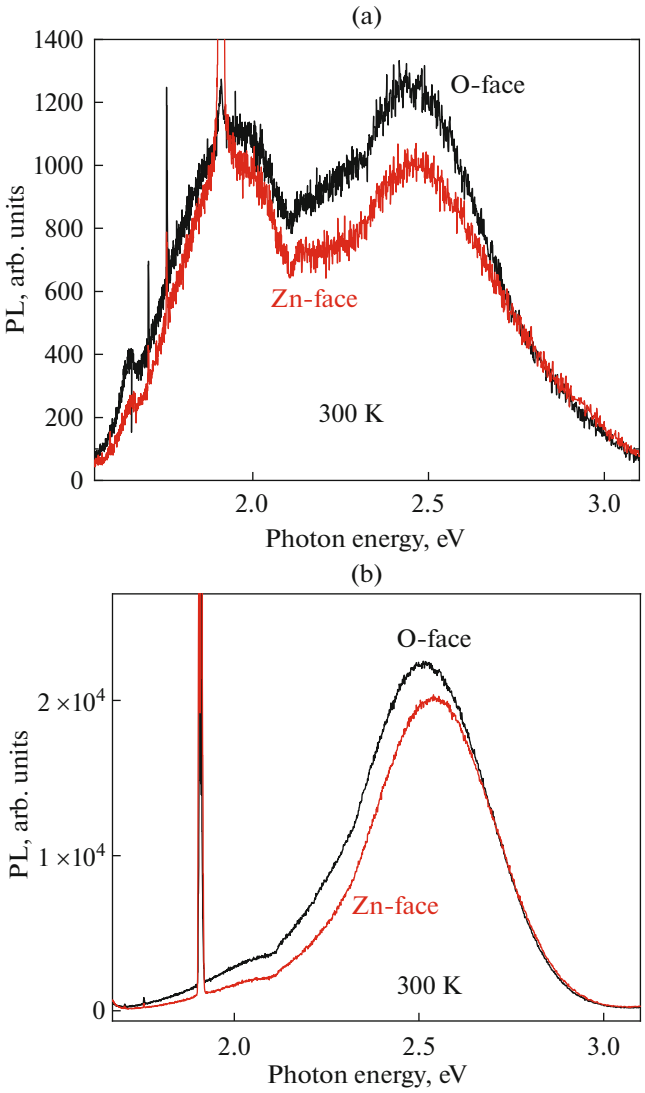

Fig. 4. *Green* and *red* bands from Zn- and O-faces of: (a) bulk ZnO crystals, and (b) those anodized at 10 V, both measured at room temperature.

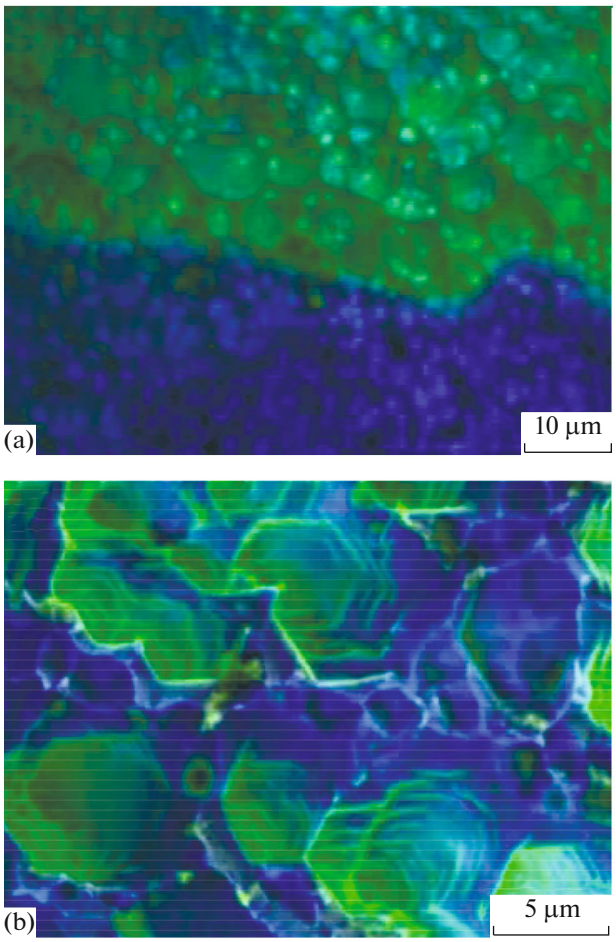

Fig. 5. CL emissions for: (a) O-face, and (b) Zn-face, both of 3.25 eV (*blue*) and of 2.35 eV (*green*) overlaid with secondary electron image of investigated area.

result, the sample with two areas containing small and large pyramids was obtained.

In the measured CL emission, the observed relationship is the same. Monte Carlo simulations using CASINO [39] indicate that CL is generated down to a depth of ~500 nm within the ZnO specimen; the majority of the signal is generated in the first ~250 nm of the specimen. The color composition of CL images (*blue* for 3.25 eV emission and *green* for 2.35 eV emission) and the corresponding secondary electron image topography were measured and presented in Fig. 5. One can see that *blue* emission dominates for the area with small pyramids (bottom of the image in Fig. 5a) while in the case of large pyramids, the *green* emission predominates (top of the image in Fig. 5a).

A similar situation is observed for the anodized Zn-face of the ZnO crystal. If produced micro-structures on the O-face have a pyramidal form, then those obtained via anodization on the Zn-face have an inversed pyramid form, as was discussed in Morphology Investigations section. The measured CL spectra for microstructures electrochemically etched on the Zn-face demonstrate a similar dependence on the produced structures sizes. The areas with deep inversed pyramids have an essential share of the *green* luminescence, in comparison to areas of shallow ones having a more share of the *blue* luminescence. Figure 5b reveals that the *blue* luminescence comes from the porous skeleton, and the *green* one is associated with a microstructured surface. The observed features of the luminescence spectra, obtained from surfaces with different morphology, can be associated either with some surface defects appeared in anodized structures, or with the size of microstructures produced by anodization. The change of the size of surface microstructures results in the change of the density of non-equilibrium charge carriers, generated by an excitation

source of luminescence, which affects the probability of various recombination channels.

The abovementioned luminescent measurements suggest a prospective application of the obtained microstructures in different optoelectronic devices. The emission efficiency enhancement allows using ZnO nanostructures as a good material with controllable luminescent properties for light emitting diodes and lasers. An enlargement of the surface after anodization of the bulk material also allows its use for solar conversion.

CONCLUSIONS

Selectivity of obtaining of ZnO microstructures with different shapes via anodization on different polar crystal surfaces was demonstrated. The obtained microstructures have a pyramidal form on the O-face, and inversed pyramids or tunnels were produced on the Zn-face. The obtained morphologies corroborate with previously reported results for wet chemical etching [23, 24]. Moreover, the size of the formed microstructures can be tuned with an applied potential during anodization. The anodization of ZnO does not generate new luminescence centers: three emission lines (*red* one located at 1.9 eV, and *green* at 2.5 eV and near edge at 3.25 eV) were observed in PL spectra. Increasing of light emission was achieved by electrochemical etching of polar ZnO crystals. For the first time, a possibility has been offered here to change the share of exciton and long-wavelength luminescence in a wide range. The received results allow concluding that the microstructured ZnO is a good material with controllable luminescent properties for light diodes and lasers.

ACKNOWLEDGMENTS

Victor Zalamai and Eduard Monaico express their thanks to the Alexander von Humboldt Foundation for support.

FUNDING

The authors acknowledge financial support from the National Agency for Research and Development, Moldova, under State Programme Project nos. 20.80009.5007.20 and 20.80009.5007.16.

AUTHOR CONTRIBUTIONS

V. Zalamai, Ed. Monaico and G. Colibaba designed the experiments; G. Colibaba synthesized the samples. Ed. Monaico and El. Monaico performed electrochemical etching and surface morphology characterization. V. Zalamai carried out photoluminescence measurements. V. Zalamai, Ed. Monaico and G. Colibaba contributed to manuscript preparation. All authors participated in the discussions. All authors have given approval to the final version of the manuscript.

REFERENCES

1. Klingshirn, C., ZnO: From basics towards applications, *Phys. Status Solidi B*, 2007, vol. 244, p. 3027. https://doi.org/10.1002/pssb.200790012
2. Pearton, S.J., Norton, D.P., Heo, Y.W., Tien, L.C., et al., ZnO spintronics and nanowire devices, *J. Electron. Mater.*, 2006, vol. 35, p. 862. https://doi.org/10.1007/BF02692541
3. Skhouni, O., El Manouni, A., Mari, B., and Ullah, H., Numerical study of the influence of ZnTe thickness on CdS/ZnTe solar cell performance, *Eur. Phys. J.: Appl. Phys.*, 2016, vol. 74, p. 24602. https://doi.org/10.1051/epjap/2015150365
4. Thomas, D.G., The exciton spectrum of zinc oxide, *J. Phys. Chem. Solids*, 1960, vol. 15, p. 86. https://doi.org/10.1016/0022-3697(60)90104-9
5. Park, Y.S., Litton, C.W., Collins, T.C., and Reynolds, D.C., Exciton spectrum of ZnO, *Phys. Rev.*, 1966, vol. 143, p. 512. https://doi.org/10.1103/PhysRev.143.512
6. Segall, B., Intrinsic absorption "edge" in II–VI semiconducting compounds with the wurtzite structure, *Phys. Rev.*, 1967, vol. 163, p. 769. https://doi.org/10.1103/PhysRev.163.769
7. Liang W.Y. and Yoffe, A.D., Transmission spectra of ZnO single crystals, *Phys. Rev. Lett.*, 1968, vol. 20, pp. 59–61. https://doi.org/10.1103/PhysRevLett.20.59
8. Klingshirn, C.F., Meyer, B.K., Waag, A., Hoffmann, A., et al., *Zinc Oxide: From Fundamental Properties towards Novel Applications*, New York: Springer-Verlag, 2010, pp. 1–120. https://doi.org/10.1007/978-3-642-10577-7
9. Ozgur, U., Alivov, Y.I., Liu, C., Teke, A., et al., A comprehensive review of ZnO materials and devices, *J. Appl. Phys.*, 2005, vol. 98, p. 041301. https://doi.org/10.1063/1.1992666
10. Meyer, B.K., Alves, H., Hofmann, D.M., Kriegseis, W., et al., Bound exciton and donor–acceptor pair recombinations in ZnO, *Phys. Status Solidi B*, 2004, vol. 241, pp. 231–260. https://doi.org/10.1002/pssb.200301962
11. Colibaba, G.V., Monaico, E.V., Goncearenco, E.P., Nedeoglo, D.D., et al., Growth of ZnCdS single crystals and prospects of their application as nanoporous structures, *Semicond. Sci. Technol.*, 2014, vol. 29, p. 125003. https://doi.org/10.1088/0268-1242/29/12/125003
12. Colibaba, G., Monaico, E.V., Goncearenco, E., Inculet, I., et al., Features of nanotemplates manufacturing on the II–VI compound substrates, in *Proc. 3rd Int. Conf. on Nanotechnologies and Biomedical Engineering (ICNBME-2015), September 23–26, 2015, Chisinau, Republic of Moldova*, IFMBE Proc. Series vol. 55, New York: Springer-Verlag, 2016, p. 188.
13. Skupiński, P., Grasza, K., Mycielski, A., Paszkowicz, W., et al., Seeded growth of bulk ZnO by chemical vapor transport, *Phys. Status Solidi B*, 2010, vol. 247, p. 1457. https://doi.org/10.1002/pssb.200983232
14. Hong, S.-H., Mikami, M., Mimura, K., Uchikoshi, M., et al., Growth of high-quality ZnO single crystals by seeded CVT using the newly designed ampoule, *J.*

Cryst. Growth, 2009, vol. 311, p. 3609.
https://doi.org/10.1016/j.jcrysgro.2009.05.015

15. Colibaba, G.V., ZnO:HCl single crystals: Thermo-dynamic analysis of CVT system, feature of growth and characterization, *Solid State Sci.*, 2016, vol. 56, p. 1. https://doi.org/j.solidstatesciences.2016.03.011
16. Colibaba, G.V., Halide-hydrogen vapor transport for growth of ZnO single crystals with controllable electrical parameters, *Mater. Sci. Semicond. Process.*, 2016, vol. 43, p. 75.
https://doi.org/10.1016/j.mssp.2015.12.005
17. Colibaba, G.V., Halide-oxide carbon vapor transport of ZnO: novel approach for unseeded growth of single crystals with controllable growth direction, *J. Phys. Chem. Solids*, 2018, vol. 116, p. 58.
https://doi.org/10.1016/j.jpcs.2018.01.009
18. Colibaba, G.V., Halide-carbon vapor transport of ZnO and its application perspectives for doping with multivalent metals, *J. Solid State Chem.*, 2018, vol. 266, p. 166.
https://doi.org/10.1016/j.jssc.2018.07.01919
19. Colibaba, G.V., Avdonin, A., Shtepliuk, I., Caraman, M., et al., Effects of impurity band in heavily doped ZnO:HCl, *Phys. B* (Amsterdam), 2019, vol. 553, p. 174.
https://doi.org/10.1016/j.physb.2018.10.031
20. Colibaba, G.V., ZnO doping efficiency by multivalent metals in complex CVT reactions, *Solid State Sci.*, 2019, vol. 97, p. 105944.
https://doi.org/10.1016/j.solidstatesciences.2019.105944
21. Colibaba, G.V., Sintering highly conductive ZnO:HCl ceramics by means of chemical vapor transport reactions. *Ceram. Int.*, 2019, vol. 45, p. 15843.
https://doi.org/10.1016/j.ceramint.2019.05.087
22. Hëupkes, J., Mëuller, J., and Rech, B., Texture etched ZnO:Al for silicon thin film solar cells, in *Transparent Conductive Zinc Oxide: Basics and Applications in Thin Film Solar Cells*, Ellmer, K., Klein, A., and Rech, B., Eds., New York: Springer-Verlag, 2008.
https://doi.org/10.1007/978-3-540-73612-7
23. Han, S.-Ch., Kim, J.-K., Kim, J.Y., Kim, K.-K., et al., Formation of hexagonal pyramids and pits on V-/VI-polar and III-/II-polar GaN/ZnO surfaces by wet etching, *J. Electrochem. Soc.*, 2010, vol. 157, p. D60.
https://doi.org/10.1149/1.3253564
24. Mehta, M. and Meier, C., Controlled etching behavior of O-polar and Zn-polar ZnO single crystals, *J. Electrochem. Soc.*, 2011, vol. 158, p. H119.
https://doi.org/10.1149/1.3519999
25. Chichibu, S.F., Sota, T., Cantwell, G., Eason, D.B., et al., Polarized photoreflectance spectra of excitonic polaritons in ZnO single crystal, *J. Appl. Phys.*, 2003, vol. 93, p. 756.
https://doi.org/10.1063/1.1527707
26. Jung, S.W., Park, W.I., Cheong, H.D., Yi, G.-Ch., et al., Time-resolved and time-integrated photoluminescence in ZnO epilayers grown on Al_2O_3 (0001) by metalorganic vapor phase epitaxy, *Appl. Phys. Lett.*, 2002, vol. 80, p. 1924.
https://doi.org/10.1063/1.1461051
27. Zhang, B.P., Binh, N.T., Segawa, Y., Wakatsuki, K., et al., Optical properties of ZnO rods formed by metalorganic chemical vapor deposition, *Appl. Phys. Lett.*, 2003, vol. 83, p. 1635.
https://doi.org/10.1063/1.1605803
28. Look, D.C., Reynolds, D.C., Litton, C.W., Jones, R.L., et al., Characterization of homoepitaxial *p*-type ZnO grown by molecular beam epitaxy, *Appl. Phys. Lett.*, 2002, vol. 81, p. 1830.
https://doi.org/10.1063/1.1504875
29. Ko, H.J., Chen, Y.F., Yao, T., Miyajima, K., et al., Bi-exciton emission from high-quality ZnO films grown on epitaxial GaN by plasma-assisted molecular-beam epitaxy, *Appl. Phys. Lett.*, 2000, vol. 77, p. 537.
https://doi.org/10.1063/1.127036
30. Yamamoto, I., Miyajima, E., Goto, T., Ko, H.J., et al., Biexciton luminescence in high-quality ZnO epitaxial thin films, *J. Appl. Phys.*, 2001, vol. 90, p. 4973.
https://doi.org/10.1063/1.1407852
31. Chen, Y., Bagnall, D.M., Zhu, Z., Sekiuchi, T., et al., Growth of ZnO single crystal thin films on *c*-plane (0001) sapphire by plasma enhanced molecular beam epitaxy, *J. Cryst. Growth*, 1997, vol. 181, p. 165.
https://doi.org/10.1016/S0022-0248(97)00286-8
32. Bagnall, D.M., Chen, Y.F., Shen, M.Y., Zhu, Z., et al., Room temperature excitonic stimulated emission from zinc oxide epilayers grown by plasma-assisted MBE, *J. Cryst. Growth*, 1998, vols. 184–185, p. 605.
https://doi.org/S0022-0248(98)80127-9
33. Zhang, X.T., Liu, Y.C., Zhi, Z.Z., Zhang, J.Y., et al., Resonant Raman scattering and photoluminescence from high-quality nanocrystalline ZnO thin films prepared by thermal oxidation of ZnS thin films, *J. Phys. D: Appl. Phys.*, 2001, vol. 34, p. 3430.
https://doi.org/10.1088/0022-3727/34/24/302
34. Tchelidze, T., Chikoidze, E., Gorochov, O., and Galtier, P., Perspectives of chlorine doping of ZnO, *Thin Solid Films*, 2007, vol. 515, p. 8744.
https://doi.org/10.1016/j.tsf.2007.04.003
35. Tian, J.-L., Zhang, H.-Y., Wang, G.-G., Wang, X.-Zh., et al., Influence of film thickness and annealing temperature on the structural and optical properties of ZnO thin films on Si (100) substrates grown by atomic layer deposition, *Superlattices Microstruct.*, 2015, vol. 83, p. 719.
https://doi.org/10.1016/j.spmi.2015.03.062
36. Janotti, A. and de Walle, C.G.V., Absolute deformation potentials and band alignment of wurtzite ZnO, MgO, and CdO, *Phys. Rev. B*, 2007, vol. 75, art. ID 121201(R).
https://doi.org/10.1103/PhysRevB.75.12120137
37. Janotti, A. and de Walle, C.G.V., Fundamentals of zinc oxide as a semiconductor, *Rep. Prog. Phys.*, 2009, vol. 72, p. 126501.
https://doi.org/10.1088/0034-4885/72/12/126501
38. Shalish, I., Temkin, H., and Narayanamurti, V., Size-dependent surface luminescence in ZnO nanowires, *Phys. Rev. B*, 2004, vol. 69, p. 245401. .
https://doi.org/10.1103/PhysRevB.69
39. Drouin, D., Couture, A.R., Joly, D., Tastet, X., Aimez, V., and Gauvin, R., CASINO V2.42: A fast and easy-to-use modeling tool for scanning electron microscopy and microanalysis users, *Scanning*, 2007, vol. 29, p. 92.
https://doi.org/10.1002/sca.20000